



Published in final edited form as:

*Anal Chem.* 2016 June 7; 88(11): 6050–6056. doi:10.1021/acs.analchem.6b01310.

## Ratiometric QD-FRET Sensing of Aqueous H<sub>2</sub>S *in vitro*

Armen Shamirian<sup>a</sup>, Hamid Samareh Afsari<sup>a</sup>, Donghui Wu<sup>b</sup>, Lawrence W. Miller<sup>a</sup>, and Preston T. Snee<sup>a,\*</sup>

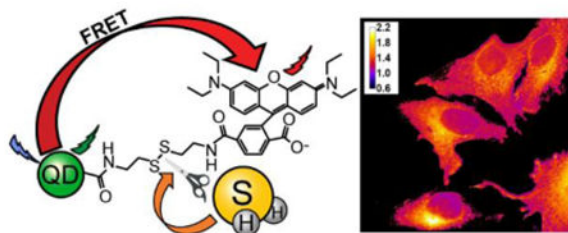
<sup>a</sup>Department of Chemistry, University of Illinois at Chicago, 845 West Taylor Street, Chicago, Illinois 60607-7061, United States

<sup>b</sup>Colgate-Palmolive Global Technology Center 909 River Road, Piscataway, NJ 08855-1343, United States

### Abstract

We report a platform for the ratiometric fluorescent sensing of the endogenously generated gaseous transmitter H<sub>2</sub>S in its aqueous form (bisulfide, or hydrogen sulfide anion) based on the alteration of Förster resonance energy transfer from an emissive semiconductor quantum dot (QD) donor to a dithiol-linked organic dye acceptor. The disulfide bridge between the two chromophores is cleaved upon exposure to bisulfide, resulting in termination of FRET as the dye diffuses away from the QD. This results in enhanced QD emission and dye quenching. The resulting ratiometric response can be correlated quantitatively to the concentration of bisulfide, and was found to have a detection limit as low as  $1.36 \pm 0.03 \mu\text{M}$ . The potential for use in biological applications was demonstrated by measuring the response of the QD-based FRET sensor microinjected into live HeLa cells upon extracellular exposure to bisulfide. The methodology used here is built upon a highly multifunctional platform that offers numerous advantages such as low detection limit, enhanced photochemical stability, and sensing ability within a biological milieu.

### Graphical abstract



H<sub>2</sub>S is a colorless, noxious and toxic gas that is mainly produced by the decomposition of organic compounds or as a byproduct from various industries.<sup>1</sup> Studies have shown that H<sub>2</sub>S is damaging to biological systems due to its high permeability through lipid membranes.<sup>2,3</sup>

\*Corresponding Author: Address correspondence to sneep@uic.edu.

Supporting Information: Additional absorption and emission spectra including calibration data, images of control samples, dynamic light scattering and NMR characterizations. The Supporting Information is available free of charge on the ACS Publications website.

**Author Contributions:** The manuscript was written through contributions of all authors. / All authors have given approval to the final version of the manuscript.

Regardless, the gas has many significant biological roles. For example, H<sub>2</sub>S has recently been recognized as an endogenously generated gaseous transmitter.<sup>4</sup> Biological production of H<sub>2</sub>S can take place via enzymatic or non-enzymatic pathways. In mammalian systems, physiological H<sub>2</sub>S levels are regulated by enzymes<sup>5, 6</sup> found in the brain and liver as well as in nervous system and vasculature tissues.<sup>7, 8</sup> The regulation of the gas has biologically beneficial effects. For example, it has been shown that H<sub>2</sub>S has antioxidant effects<sup>9</sup> and is an anti-inflammatory agent.<sup>10</sup> H<sub>2</sub>S levels are also associated with cardioprotective and anti-apoptotic effects,<sup>11-13</sup> the regulation of vascular tension, and controlling blood pressure.<sup>14, 15</sup> However, recent studies have indicated that H<sub>2</sub>S levels are related to diseases such as cancer,<sup>16</sup> Down syndrome,<sup>17</sup> and Alzheimer's disease.<sup>18</sup>

There is an ongoing debate concerning the concentration of hydrogen sulfide in cells, blood, and in tissues. A wide range of 2-300 μM has been reported by different groups,<sup>19-23</sup> which is likely the result of the use of different sampling techniques and detection methods. Concentrations in the nanomolar range have also been reported.<sup>24</sup> This is unfortunate as the biological effects of H<sub>2</sub>S depends on its concentration, as the gas is cytoprotective at lower levels while it is cytotoxic and causes apoptosis in human cells at higher concentrations. Furthermore, to function as a gaseous transmitter the intracellular concentration of H<sub>2</sub>S has to be high to activate the signaling mechanism, but it is consumed quickly to maintain the whole tissue concentration at safe lower levels.<sup>24</sup>

The development of a reliable and efficient method for the detection of the H<sub>2</sub>S in biological environments has a crucial importance to understand its role in many pathologies. Methods of H<sub>2</sub>S detection such as chromatography, colorimetry, and electrochemical assays,<sup>25, 26</sup> suffer from poor biological compatibility, and require complicated sample preparation processes. One strategy to address these issues is based on the fact that H<sub>2</sub>S dissociates in aqueous solution to form an equilibrium between  $\text{H}_2\text{S} \leftrightarrow \text{HS}^- \leftrightarrow \text{S}^{2-}$ , where bisulfide (HS<sup>-</sup>, or hydrogen sulfide) is favored and is the target analyte “stand-in” for H<sub>2</sub>S. As such, the design of fluorescent probes for bisulfide have attracted significant attention due to the convenience, compatibility, and sensitivity of fluorescence methods that facilitate the real-time detection of the analyte within biological environments. Sulfide-reactive fluorescent probes have been designed based on different strategies such as metal-sulfide interaction, reduction of azide and nitro groups, and nucleophilic addition; detailed mechanisms and discussion of these systems can be found in recent reviews.<sup>27, 29</sup> Most of the reported probes are single-emission turn-on sensors that can be difficult to quantify in a complex biological environment. A ratiometrically responsive (i.e. color-changing and thus self-calibrating) sensor addresses this problem, although there are few reports of such.<sup>30, 32</sup> Herein, we report a novel design of a QD-based energy-transfer sensor for detection of bisulfide ion in solution. The response mechanism is based on the reducing ability of the ion that can cleave the disulfide bond connecting the QD to dye. The action of the ion results in a loss of FRET between green emitting QD donor and rhodamine dye acceptor that produces a ratiometric fluorescence response to the presence of HS<sup>-</sup>.

## Experimental Section

### Materials and Instrumentation

1,2,4-benzenetricarboxylic anhydride (97%), 3-diethylaminophenol (97%), 4-(dimethylamino) pyridine (DMAP, 98%), DL-dithiothreitol (>98%), D-(+)-glucose (>99.5%), L-cysteine (97%), L-glycine (>98.5%), L-lysine (>98%), potassium bisulfate (99%), trimethylamine (TEA, 99%), zinc chloride (98%), and high molecular weight polyvinyl chloride were purchased from Sigma-Aldrich. Glutathione (reduced, 98%), sodium sulfide nonahydrate (>98%), and N,N'-disuccinimidyl carbonate (DSC, 98%) were purchased from Acros. Sodium sulfate (anhydrous, >99%), sodium sulfite (anhydrous, >98%), and sodium thiosulfate pentahydrate (99.5%) were purchased from Fisher Chemicals. Sodium thiocyanate (98%) was purchased from Alfa Aesar. Mono-t-boc-cystamine-HCl was purchased from Fisher Scientific. Bis(2-ethylhexyl)sebacate (98%) was purchased from TCI America. The QD-functionalization reagent methoxypolyethylene glycol 350 carbodiimide (MPEG 350 CD),<sup>33</sup> Rhodamine B piperazine,<sup>34</sup> and 40% octylamine-modified poly(acrylic acid) (PAA)<sup>35</sup> were prepared according to previously published protocols. <sup>1</sup>H NMR spectra were recorded on a Bruker Avance DRX 400 NMR spectrometer. UV-vis absorbance spectra of the samples were taken using a Varian Cary 300 Bio UV/vis spectrophotometer, and fluorescence emission spectra were obtained using a custom-designed Horiba Jobin Yvon FluoroLog spectrophotometer. Dynamic light scattering (DLS) experiments were performed on a Malvern Zetasizer Nano. HeLa cells (CCL-2) were purchased from American Type Culture Collection. Dulbecco's modified eagle medium (DMEM, 10-014 CV) and 0.25% trypsin/2.21 mM EDTA were purchased from Corning Cellgro<sup>®</sup>. MEM non-essential amino acids (11140) and HEPES (15630-080) were purchased from Gibco<sup>®</sup>. Micropipette preparation glass bottom culture dishes (P50G-1.5-14-F) were purchased from Matek Corporation (Ashlan, MA). Xenoworks<sup>TM</sup> Microinjection Systems, P-1000 pipette puller and borosilicate glass tubes (BF100-78-10) were used for microinjections (Sutter Instruments, Novato, CA).

### Bisulfide-reactive Carboxyrhodamine B Synthesis

The bisulfide-reactive rhodamine B derivative used in this study was synthesized following the outline in Scheme 2.

### Synthesis of Carboxyrhodamine B (3)

A mixture of 3-diethylaminophenol **1** (1.03g, 6.05 mmol), and 1,2,4-benzenetricarboxylic anhydride **2** (0.6 g, 3.02 mmol) was heated to 195 °C in the presence of a catalytic amount of ZnCl<sub>2</sub> under a nitrogen atmosphere for 1 h. The resulting red mixture was cooled to room temperature, and dissolved in 5% NaOH solution. The mixed isomers of carboxyrhodamine B were precipitated out of the solution by acidification using HCl (pH=1). 5- and 6-carboxyrhodamine B **4** isomers were separated as TEA salts by flash chromatography (DCM:MeOH:TEA 4:1:0.5).<sup>36</sup> Solvents were evaporated under reduced pressure. Each isomer was dissolved in ETOAc (40 mL), and washed with 1M KHSO<sub>4</sub> (3×30 mL), brine (30 mL), and dried over anhydrous Na<sub>2</sub>SO<sub>4</sub> to obtain pure 5-carboxyrhodamine B (575 mg, 39%), and 6-carboxyrhodamine B (452 mg, 30%). <sup>1</sup>H NMR data are shown in Figure S1 of the supporting information.

### Synthesis of 6-Carboxytetraethylrhodamine N-Hydroxysuccinimide ester (6)

6-carboxyrhodamine B **5** (100 mg, 0.2 mmol), DMAP (122 mg, 1 mmol), and TEA (140  $\mu$ L, 1 mmol) were dissolved in dry DCM (10 mL). DSC (105 mg, 0.4 mmol) was added, and the mixture was stirred under nitrogen atmosphere at room temperature for 1 h. After 1 h the reaction was quenched by addition of AcOH (120  $\mu$ L, 2 mmol), and the final product was purified by flash chromatography using 1% AcOH in acetone followed by MeOH:DCM:AcOH (9:89:2) as eluent (65% yield).  $^1\text{H}$  NMR data are shown in Figure S2 of the supporting information.

Synthesis of N-(2-((2-aminoethyl)disulfanyl)ethyl)-3',6'-bis(diethylamino)-3-oxo-3H-spiro [isobenzofuran-1,9'-xanthene]-6-carboxamide (**8**). 6-carboxytetraethylrhodamine N-hydroxysuccinimide ester **6** (58.4 mg, 0.1 mmol), mono-t-boc-cystamine-HCl (28.81 mg, 0.1 mmol), and TEA (14  $\mu$ L, 0.1 mmol) were dissolved in dry DCM, and stirred under nitrogen atmosphere at room temperature over night. The next day the solvent was evaporated under reduced pressure, and the resulting residue was purified by flash chromatography (DCM:MeOH 85:15) to obtain compound **7**. For boc deprotection, the resulting compound was dissolved in DCM (4 mL), and then  $\text{CF}_3\text{COOH}$  (2 mL) was added. After the mixture was stirred for 2 h under a nitrogen atmosphere at room temperature, the solvent was evaporated under reduced pressure. The product was purified by flash chromatography (DCM:MeOH:TEA 4:1:0.5) to obtain compound **8** (81% yield). Optical and  $^1\text{H}$  NMR data are shown in Figures S3, S4a of the supporting information.

### QDs Synthesis, PVC Modification, and Water Solubilization

CdSe/CdZnS core/shell QDs were synthesized according to previously published protocols.<sup>37</sup> Approximately 0.5 g of the crude sample was processed by addition of a small amount of isopropanol followed by methanol to induce flocculation. The supernatant was discarded, and the precipitate was dried under vacuum. The QDs were dissolved in 2 mL of THF, and 50  $\mu$ L of a PVC coating solution<sup>38</sup> (50 mg high molecular weight polyvinyl chloride and 100 mg of bis(2-ethylhexyl) sebacate dissolved in 5 mL of THF) was added. The mixture was stirred gently overnight, after which the solvent was evaporated under reduced pressure. Next, 65 mg of amphiphilic 40% octylamine-modified PAA was added to the QDs followed by  $\sim$ 3 mL of dry THF. The solution was sonicated for several minutes to dissolve the polymer completely. We believe that the hydrophobic portions of the polymer coordinate to pores in the PVC coating,<sup>39</sup> which is why the QDs dispersed into 0.1 M NaOH solution after the solvent was evaporated under reduced pressure. The solution was dialyzed to neutrality to remove excess polymer. The solution was then filtered through a 0.2  $\mu$ m syringe filter to yield a monodisperse plastic-coated water-soluble QD solution. The fact that the materials passed through the filter and remained colloidally stable indicated that the materials were not agglomerated. Samples without PVC modification were prepared by repeating the procedure above without the addition of the PVC coating solution. These materials were used in cell imaging studies. As such, their quantum yield was measured to be 0.54 vs. fluorescein,<sup>40</sup> see Figure S4b of the supporting information.

### Compound 8 Dye Conjugation to QDs

A solution of ~5 mg of MPEG 350 CD dissolved in 0.5 mL of water-solubilized CdSe/CdZnS QDs ( $1.24 \times 10^{-6}$  M) was stirred for 30 min. Next, a sub-milligram quantity of compound 8 was dissolved in pH 8 phosphate buffer and was added drop-wise to the activated QD solution until the dye emission appeared to slightly dominate the dots under illumination with a black light. Next, 2 mL of pH 8 phosphate buffer was added, and the reaction was allowed to stir overnight. The next day, dialysis was performed using centrifugation filters to remove excess unreacted dye. The QD sulfide sensor solution was then diluted to working concentration of  $3.43 \times 10^{-8}$  M using pH 7.4 Tris-HCl buffer. The conjugation yield for the unmodified (PVC free) dots was calculated to be 42% by comparing absorbance spectra before and after dialysis, and the number of the dye per QD was determined to be 1.3 based on the absorptivity of the dye component.

These data are shown in Figure S5 of the supporting information. The characteristic FRET distance ( $R_0$ ) was determined to be 5.95 nm using the methods outlined in ref. 37. Furthermore, the FRET efficiency was determined to be >70% for both plastic coated and unmodified water-soluble QD/dye conjugates based on the quenching of the donor fluorescence intensity shown in Figure S6. The high efficiency observed in the PVC modified QDs is surprising given the hydrodynamic radius determined from DLS measurements. We hypothesize that the porous nature of the PVC coating, due to the addition of the plasticizer,<sup>39</sup> allows the dye to interpolate within the coating such that FRET efficiency is enhanced.

### Cell Culture

HeLa cells were maintained in DMEM (+) (DMEM supplemented with 10% FBS, 1× MEM non-essential amino acids and 15 mM HEPES) at 37 °C and 5% CO<sub>2</sub>. The cells were passaged with 0.25% trypsin/2.21 mM EDTA.

### Microinjection and Fluorescence Microscopy

HeLa cells were grown to 60-70% confluency in a glass bottom dish before microinjection. Micropipettes were prepared by the following parameters: heat, ramp-42; pull, 80; velocity 30; time 100; and pressure, 400. Micropipettes were loaded with the sensor solution by capillary action and the solution was injected into the cytosol by using the following microinjector parameters: transfer pressure: 15 hPa; injection width, 0.2 sec; injection pressure 3000 hPa. Fluorescence images of the injected cells were acquired after 20 min using an epi-fluorescence microscope (Axiovert 200, equipped with AxioCam MRm CCD camera and Axiovision software (V 4.6.1.0), Carl Zeiss, Inc.) modified with a UV LED emitting at 365 nm (UV-LED-365, Prizmatix, Ltd.). All images were obtained with a 63×/1.25 N.A. EC Plan Neofluar oil-immersion objective (Carl Zeiss, Inc.) and G365 excitation filter. Emission filters ( $535 \pm 25$  nm and  $610 \pm 37.5$  nm) were used to separately image and measure the quantum dot and dye emission intensities. The same settings were used to acquire images before and after the addition of sodium sulfide solution. All images are dark current corrected. Signal intensity was determined from ROIs in the cytoplasm using the Image J software (v 1.47) package.<sup>41</sup>

## Results and Discussion

Considering the equilibrium  $pK_a \sim 7.0$  for  $H_2S \leftrightarrow HS^-$  and the significantly higher  $pK_{a2}$  of  $HS^- \leftrightarrow S^{2-}$ ,<sup>42</sup> it is not surprising that the  $H_2S / HS^-$  ratio within the cells is believed to be equal, and that almost 80% of the  $H_2S$  is in the form of anionic state in extracellular fluid and plasma. Furthermore,  $HS^-$  is a stronger nucleophile compared to cysteine, glutathione, and other anions such as chloride and hydroxide. This feature can be utilized for selective sensing of  $H_2S$  via a nucleophilic displacement mechanism of  $HS^-$  under biological conditions.

The wide variation in reported concentration levels discussed above is likely due to the choice of technique and approach. The employment of harsh chemical conditions for analyte extraction and sampling may alter the quantity of sulfur containing species. Moreover, technical limitations involved in some methods result in indirect detection of  $H_2S$ . Regardless, the employment of reactive fluorescent probes has advantages, including minimal sample preparation, direct visualization of the analyte, high sensitivity and (possibly) low detection limit, and non-destructive detection in biological environments.<sup>43</sup> Concerning fluorescence-based sensing, activation of a chromophore by an analyte provides a relatively background-free signal that is easy to interpret. However, one cannot ascertain the effect of analyte concentration within a complex environment such as a cell. For example, if no emission is observed from a cell nucleus, is that because no analyte is present or due to the fact that the probe did not diffuse through the nuclear membrane?

These issues are addressed by the use of ratiometrically reporting chromophores, which change color in the presence of the analyte. As a result, the spectrum of the probe provides the analytical metric, rather than the fluorescent probe intensity. Ratiometric fluorescent sensors can be prepared by conjoining a donor / acceptor pair of chromophores that engage in FRET, the efficiency of which is altered by the action of the analyte. Such sensitivity can be imparted by cleavage of the donor-acceptor link by the activity of the analyte that results in the termination of the energy transfer. As such, the emission of the donor becomes more dominant, which alters the integrated emission ratio.<sup>44, 45</sup> Since cleavage of a disulfide bond by  $HS^-$  is facile, linking a dye to a QD via a disulfide bond can be incorporated within a ratiometric fluorescent sensing strategy. To this end we have synthesized a carboxyrhodamine B derivative with an amine-terminated linker containing a disulfide bond. This chromophore can act as an acceptor for a green-emitting water-soluble quantum dot donor after carbodiimide coupling the two together (Scheme 1); see Figure S6 & S7 of the supporting information for spectroscopic data. The disulfide bond cleaves upon exposure to  $HS^-$ , causing the dye to diffuse away from the QD and terminating FRET. This was confirmed by measuring the filtrate of samples that were exposed to  $Na_2S$  solution after dialysis, see Figure S8.

The system was tested using freshly-prepared sodium sulfide in pH 7.4 Tris-HCl buffer solution to represent an  $H_2S$  source. The fluorescent response of the sensor shown in Figure 1a was quantified by fitting multiple Gaussian functions to the sulfide-dependent emission spectra to separate the QD and dye components. The integrated emission ratio of the QD:dye was plotted as a function of the  $HS^-$  concentration (Figure 1a), which shows a linear



correlation. The detection limit was determined to be  $21.6 \pm 0.4 \mu\text{M}$  using the bootstrap method.<sup>46</sup> Note that the detection limit of ratiometric sensors is scalable with concentration to within reasonable limits as determined by the detection efficiency. As such, the sensor was diluted by 10 $\times$ , reanalyzed, and was found to have a detection limit of  $1.36 \pm 0.03 \mu\text{M}$  using the data shown in Figure 1b. To study the selectivity, the ratiometric response of the QD-dye complex was measured after exposure to various thiols and amino acids in pH 7.4 Tris-HCl

Several control experiments were conducted to investigate the mechanism of sensing and identify possible pitfalls of the method. For example, a Rhodamine B derivative was used as the organic chromophore as it was believed to have a minimal intrinsic sensitivity to environmental factors. However, an amide bond-coupled (and thus non-sulfide reactive) QD/Rhodamine B piperazine chromophore responded to bisulfide ion in a nearly-identical manner to that observed in the QD/bisulfide-reactive dye system (see Figure S9 of the supporting information). Further investigation revealed that the absorption of Rhodamine B piperazine is suppressed when titrated with HS<sup>-</sup> (Figure S10a), which would result in a ratiometric response in the coupled chromophore due to a modulation of the FRET efficiency. The response shows a linear correlation between the integrated QD:dye emissions ratio versus HS<sup>-</sup> concentration to 150  $\mu\text{M}$  of bisulfide under the conditions employed. The response saturated above this range, which was not true for the reduction-sensitive FRET system discussed above. This is likely due to the difference in analyte recognition mechanisms; regardless, the amide-bonded coupled chromophore was not used in further studied due to this limitation.

Given that Rhodamine B was found to have an intrinsic response to the presence of the analyte, we also investigated the absorption of the bisulfide-reactive carboxyrhodamine dye due to exposure to Na<sub>2</sub>S and found an even stronger response as shown in Figure S10b. These data suggest that the ratiometric response of the sensor shown in Figure 1 may be due to both dye cleavage and suppression of the dye's absorptivity. However, cleavage of the QD-dye linker must ultimately be responsible for the observations due to the lack of saturation behavior and the irreversibility of the reaction.

While Figure 1a shows that the emission of the QD/bisulfide-reactive carboxyrhodamine B dye has a clean response to bisulfide exposure with a clear isosbestic point appearing at  $\sim 570 \text{ nm}$ , the absolute intensity of the sensor's emission was reduced as seen in the unnormalized spectra in Figure S11a. It was determined that the overall loss of fluorescence efficiency was due to bisulfide quenching of the QD donor component. As such, several avenues were explored to protect the QD from quenching by the analyte, one of which was to coat the QDs with polyvinyl chloride (PVC) before water solubilization with 40% octylamine-modified poly(acrylic acid). These water soluble, "plastic-coated" QDs were conjugated to the bisulfide-reactive carboxyrhodamine B dye and were then titrated with bisulfide solution. The emission and linear response of this sensor are shown in Figure S11b, where it can be seen that the plastic coating reduced quenching of the QDs due to HS<sup>-</sup> exposure. The ratiometric response to bisulfide was linear (Figure S12) with a detection limit of  $41.9 \pm 0.3 \mu\text{M}$ ; in fact these data appear nearly identical to that shown in Figure 1. However, DLS results shown in Figure S13 reveal that the plastic-coated QDs are  $\sim 150 \text{ nm}$

in diameter which is a significant increase from  $\sim 8.5$  nm observed in un-modified water-soluble dots. Furthermore, these dots did not diffuse freely and distribute themselves evenly in live cells after microinjection, most likely due to their large size. As a result, these samples were not examined further, and all experiments with sulfide sensing in live cells were performed using sensors that were not modified with PVC coating.

The efficacy of the sensor in live cells was investigated. HeLa cells were microinjected with  $\sim 1.5$   $\mu\text{mol}$  of the QD/bisulfide-reactive carboxyrhodamine dye and were incubated for 5 min. Wavelength-selective microscopic images were obtained using  $535 \pm 25$  nm and  $610 \pm 37.5$  nm bandpass filters for the QD and dye channels, respectively. Next, the cells were treated with a 200  $\mu\text{M}$  bisulfide solution for an additional 20 min, after which time they were re-imaged as shown in Figure 3. The detailed changes in the intensities of the QD and dye signals are quantified in Table S1. The average enhancement in the intensity of the QD signal (+17%) and quenching of dye intensity (-29%) confirms the potential use of the ratiometric sensor for the detection of bisulfide in biological environments. To verify that the enhancement in the QDs' emission was due to FRET modulation, HeLa cells were microinjected with water-soluble QDs and were imaged before and after sulfide solution exposure in the same manner as discussed above (Figure S14). The results showed a drop in intensity of the QD emission (-9%). This confirms that the ratiometric response observed in the cells was not due to a singular, intrinsic response of QDs due to  $\text{Na}_2\text{S}$  exposure.

We attempted to quantify the *in vitro* data by comparing them to the calibration curve shown in Figure S15 generated by measuring the emission of the sensor in liquid drops of bisulfide standards using the same microscope system. Unfortunately, the *in vitro* data is not sensibly consistent with this calibration with regard to the observed QD:dye emission ratios and the magnitude of response due to exposure to 200  $\mu\text{M}$  of the analyte. This result was not entirely unexpected as previous attempts to quantitatively measure the pH in tumor microenvironments using QD-based ratiometric sensors was found to be similarly problematic.<sup>40</sup> As such, it is likely that quantitative biological measurements require the use of calibration standards that have similar chemical and biological composition as the sample.

## Conclusion

In conclusion, a QD-based FRET platform has been developed for sensing aqueous bisulfide ions within biological environments. The probe has a detection limit of  $1.36 \pm 0.03$   $\mu\text{M}$  in buffer and is selective towards HS<sup>-</sup> compared to the other thiols including amino acids. The self-calibrating response of the sensor, in addition to the positive qualities of QDs such as high quantum yield and photostability, make this probe a unique tool for the qualitative detection of the  $\text{H}_2\text{S}$  (via aqueous bisulfide) concentration changes in complex biological matrices.

## Supplementary Material

Refer to Web version on PubMed Central for supplementary material.



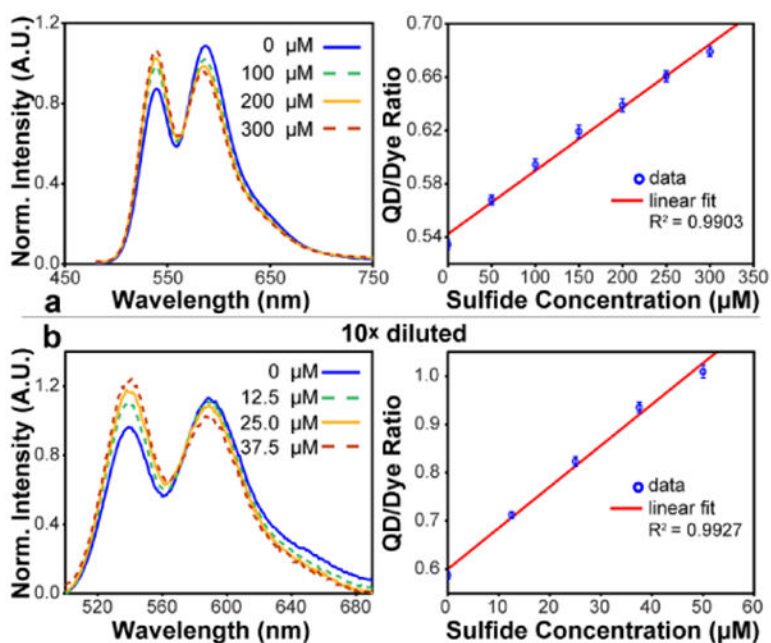
## Acknowledgments

We would like to thank Roohollah Kazem Shiroodi for helpful discussions. PTS would like to thank support by Colgate-Palmolive, the Chicago Biomedical Consortium with support from the Searle Funds at the Chicago Community Trust, as well as the University of Illinois at Chicago. LWM was supported by the National Institutes of Health (R01GM081030).

## References

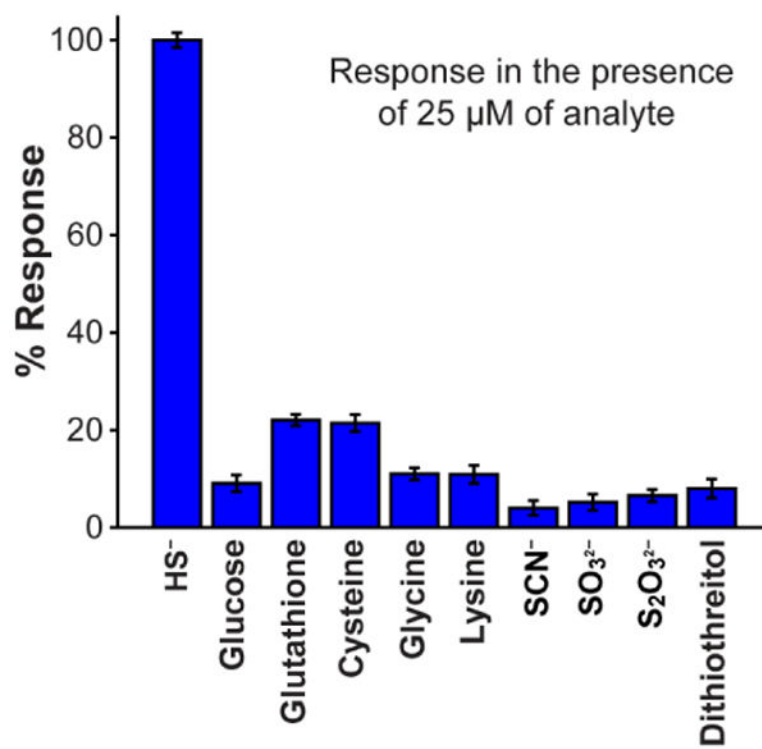
1. Skrtic, L. Master's Degree Thesis. University of California; Berkeley, CA: 2006. Hydrogen Sulfide, Oil and Gas, and People's Health.
2. Cuevasanta E, Denicola A, Alvarez B, Moller MN. PLoS One. 2012; 7:e34562. [PubMed: 22509322]
3. Reiffenstein RJ, Hulbert WC, Roth SH. Annu Rev Pharmacol Toxicol. 1992; 32:109–134. [PubMed: 1605565]
4. Gadalla MM, Snyder SH. J Neurochem. 2010; 113:14–26. [PubMed: 20067586]
5. Kimura H. Amino Acids. 2011; 41:113–121. [PubMed: 20191298]
6. Wang R. Physiol Rev. 2012; 92:791–896. [PubMed: 22535897]
7. Chen X, Jhee KH, Kruger WD. J Biol Chem. 2004; 279:52082–52086. [PubMed: 15520012]
8. Shibuya N, Tanaka M, Yoshida M, Ogasawara Y, Togawa T, Ishii K, Kimura H. Antioxid Redox Signal. 2009; 11:703–714. [PubMed: 18855522]
9. Sagara Y, Schubert D. J Neurosci. 1998; 18:6662–6671. [PubMed: 9712638]
10. Fiorucci S, Antonelli E, Distrutti E, Rizzo G, Mencarelli A, Orlandi S, Zanardo R, Renga B, Di Sante M, Morelli A, Cirino G, Wallace JL. Gastroenterology. 2005; 129:1210–1224. [PubMed: 16230075]
11. Calvert JW, Jha S, Gundewar S, Elrod JW, Ramachandran A, Pattillo CB, Kevil CG, Lefer DJ. Circ Res. 2009; 105:365–374. [PubMed: 19608979]
12. Lavu M, Bhushan S, Lefer DJ. Clin Sci (Lond). 2011; 120:219–229. [PubMed: 21126235]
13. Sodha NR, Clements RT, Feng J, Liu Y, Bianchi C, Horvath EM, Szabo C, Sellke FW. Eur J Cardiothorac Surg. 2008; 33:906–913. [PubMed: 18314343]
14. Zhao W, Zhang J, Lu Y, Wang R. EMBO J. 2001; 20:6008–6016. [PubMed: 11689441]
15. Yang G, Wu L, Jiang B, Yang W, Qi J, Cao K, Meng Q, Mustafa AK, Mu W, Zhang S, Snyder SH, Wang R. Science. 2008; 322:587–590. [PubMed: 18948540]
16. Wu D, Si W, Wang M, Lv S, Ji A, Li Y. Nitric Oxide. 2015; 50:38–45. [PubMed: 26297862]
17. Kamoun P, Belardinelli MC, Chabli A, Lallouchi K, Chadefaux-Vekemans B. Am J Med Genet A. 2003; 116a:310–311. [PubMed: 12503113]
18. Eto K, Asada T, Arima K, Makifuchi T, Kimura H. Biochem Biophys Res Commun. 2002; 293:1485–1488. [PubMed: 12054683]
19. Kabil O, Banerjee R. J Biol Chem. 2010; 285:21903–21907. [PubMed: 20448039]
20. Olson KR. Biochim Biophys Acta. 2009; 1787:856–863. [PubMed: 19361483]
21. Han Y, Qin J, Chang X, Yang Z, Du J. Cell Mol Neurobiol. 2006; 26:01–107.
22. Goodwin LR, Francom D, Dieken FP, Taylor JD, Warenycia MW, Reiffenstein RJ, Dowling G. J Anal Toxicol. 1989; 13:105–109. [PubMed: 2733387]
23. Hyspler R, Ticha A, Indrova M, Zadak Z, Hysplerova L, Gasparic J, Churacek J. J Chromatogr B Analyt Technol Biomed Life Sci. 2002; 770:255–259.
24. Furne J, Saeed A, Levitt MD. Am J Physiol Regul Integr Comp Physiol. 2008; 295:R1479–1485. [PubMed: 18799635]
25. Ubuka T. J Chromatogr B Analyt Technol Biomed Life Sci. 2002; 781:227–249.
26. Kraus, DW.; Doeller, JE.; Zhang, X. Electrochemical Sensors for the Determination of Hydrogen Sulfide Production in Biological Samples. In: Zhang, X.; Ju, H.; Wang, J., editors. Electrochemical Sensors, Biosensors and Their Biomedical Applications. Academic Press, Inc.; San Diego, CA, USA: 2008. p. 213-235.

27. Guo Z, Chen G, Zeng G, Li Z, Chen A, Wang J, Jiang L. *Analyst*. 2015; 140:1772–1786. [PubMed: 25529122]
28. Peng H, Chen W, Cheng Y, Hakuna L, Strongin R, Wang B. *Sensors (Basel)*. 2012; 12:15907–15946. [PubMed: 23202239]
29. Lin VS, Chen W, Xian M, Chang CJ. *Chem Soc Rev*. 2015; 44:4596–4618. [PubMed: 25474627]
30. He L, Lin W, Xu Q, Wei H. *Chem Commun (Camb)*. 2015; 51:1510–1513. [PubMed: 25502568]
31. Strianese M, Palm GJ, Milione S, Kuhl O, Hinrichs W, Pellicchia C. *Inorg Chem*. 2012; 51:11220–11222. [PubMed: 23072298]
32. Kar C, Adhikari MD, Ramesh A, Das G. *Inorg Chem*. 2013; 52:743–752. [PubMed: 23302031]
33. Shen H, Jawaid AM, Snee PT. *ACS Nano*. 2009; 3:915–923. [PubMed: 19275175]
34. Nguyen T, Francis MB. *Org Lett*. 2003; 5:3245–3248. [PubMed: 12943398]
35. Chen Y, Thakar R, Snee PT. *J Am Chem Soc*. 2008; 130:3744–3745. [PubMed: 18321112]
36. Brunet A, Aslam T, Bradley M. *Bioorg Med Chem Lett*. 2014; 24:3186–3188. [PubMed: 24856065]
37. Snee PT, Tyrakowski CM, Page LE, Isovich A, Jawaid AM. *J Phys Chem C*. 2011; 115:19578–19582.
38. Dubach JM, Harjes DI, Clark HA. *J Am Chem Soc*. 2007; 129:8418–8419. [PubMed: 17567136]
39. Maeda Y, Paul DR. *J Polym Sci Part B Polym Phys*. 1987; 25:1005–1016.
40. Porres L, Holland A, Palsson LO, Monkman AP, Kemp C, Beeby A. *J Fluoresc*. 2006; 16:267–272. [PubMed: 16477506]
41. Schneider CA, Rasband WS, Eliceiri KW. *Nat Methods*. 2012; 9:671–675. [PubMed: 22930834]
42. Li Q, Lancaster JR Jr. *Nitric Oxide-Biol Ch*. 2013; 35:21–34.
43. Ntziachristos V, Ripoll J, Wang LV, Weissleder R. *Nat Biotechnol*. 2005; 23:313–320. [PubMed: 15765087]
44. Yuan L, Lin W, Zheng K, Zhu S. *Acc Chem Res*. 2013; 46:1462–1473. [PubMed: 23419062]
45. Shamirian A, Ghai A, Snee PT. *Sensors (Basel)*. 2015; 15:13028–13051. [PubMed: 26053750]
46. Efron B. *Ann Stat*. 1979; 7:1–26.
47. Lemon CM, Curtin PN, Somers RC, Greytak AB, Lanning RM, Jain RK, Bawendi MG, Nocera DG. *Inorg Chem*. 2014; 53:1900–1915. [PubMed: 24143874]

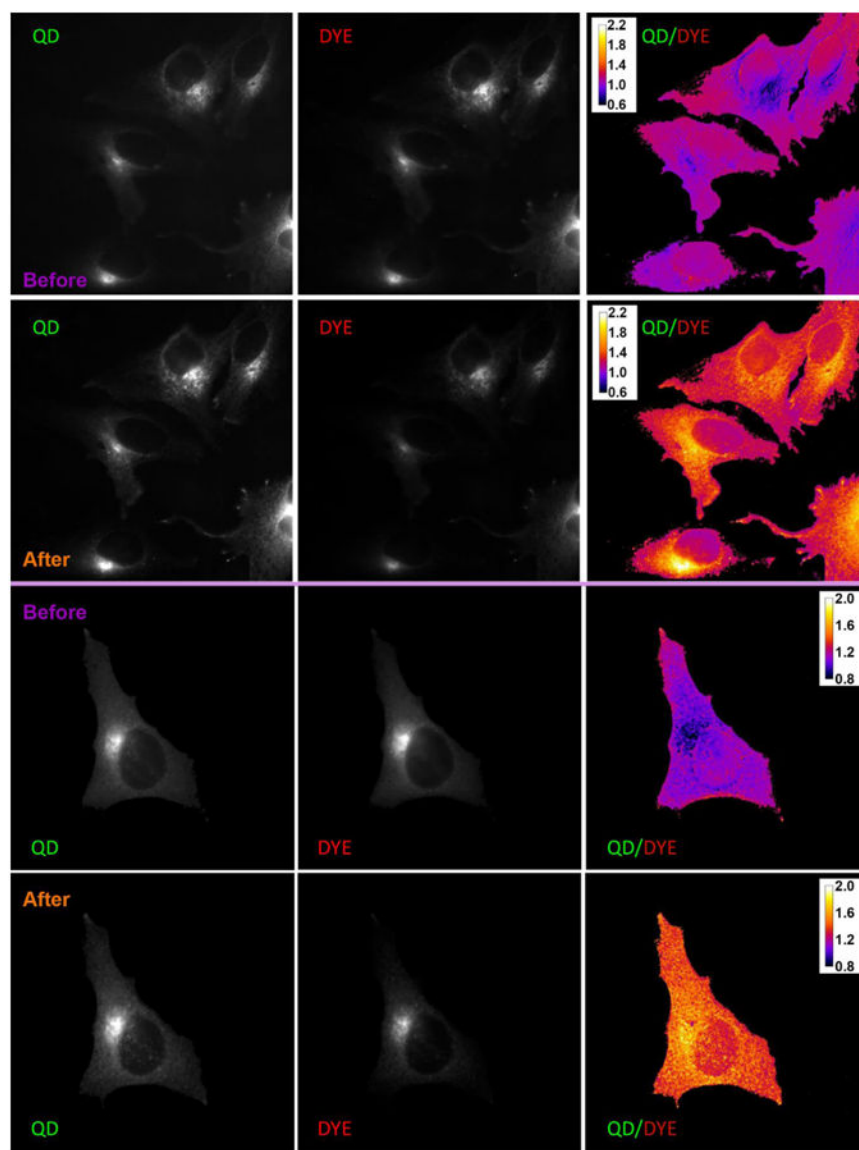


**Figure 1.**

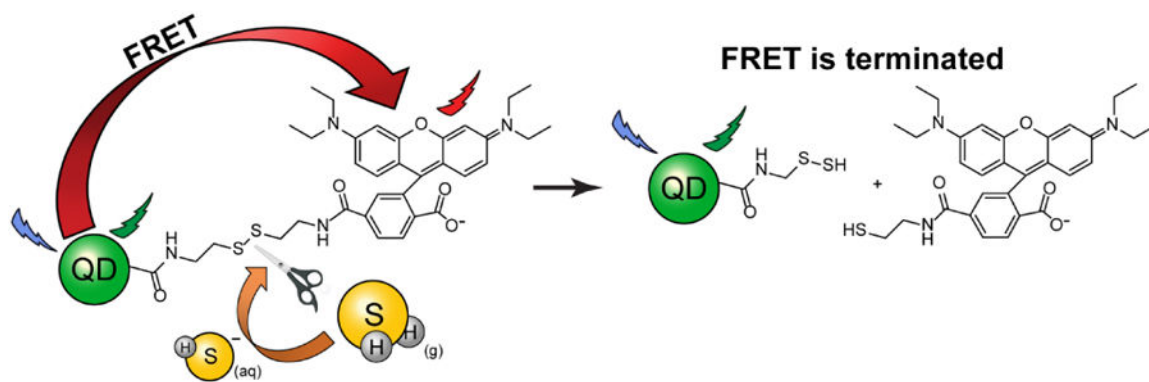
(A) Normalized emission of the coupled QD/bisulfide-reactive carboxyrhodamine dye (compound 8) sensor ( $3.4 \times 10^{-8}$  M) upon exposure to  $\text{HS}^-$ . Also the ratio of the integrated emission of the QD donor over the dye acceptor as a function of  $\text{HS}^-$  concentration reveals a  $21.6 \pm 0.4$   $\mu$ M detection limit. (B) The same for the QD/bisulfide-reactive carboxyrhodamine dye sensor at  $10\times$  dilution ( $3.4 \times 10^{-9}$  M) reveals a lower detection limit of  $1.36 \pm 0.03$   $\mu$ M.



**Figure 2.** Fluorescence intensity ratio change in response to various relevant analytes (25  $\mu\text{M}$ ). The data are normalized against the response to bisulfide.

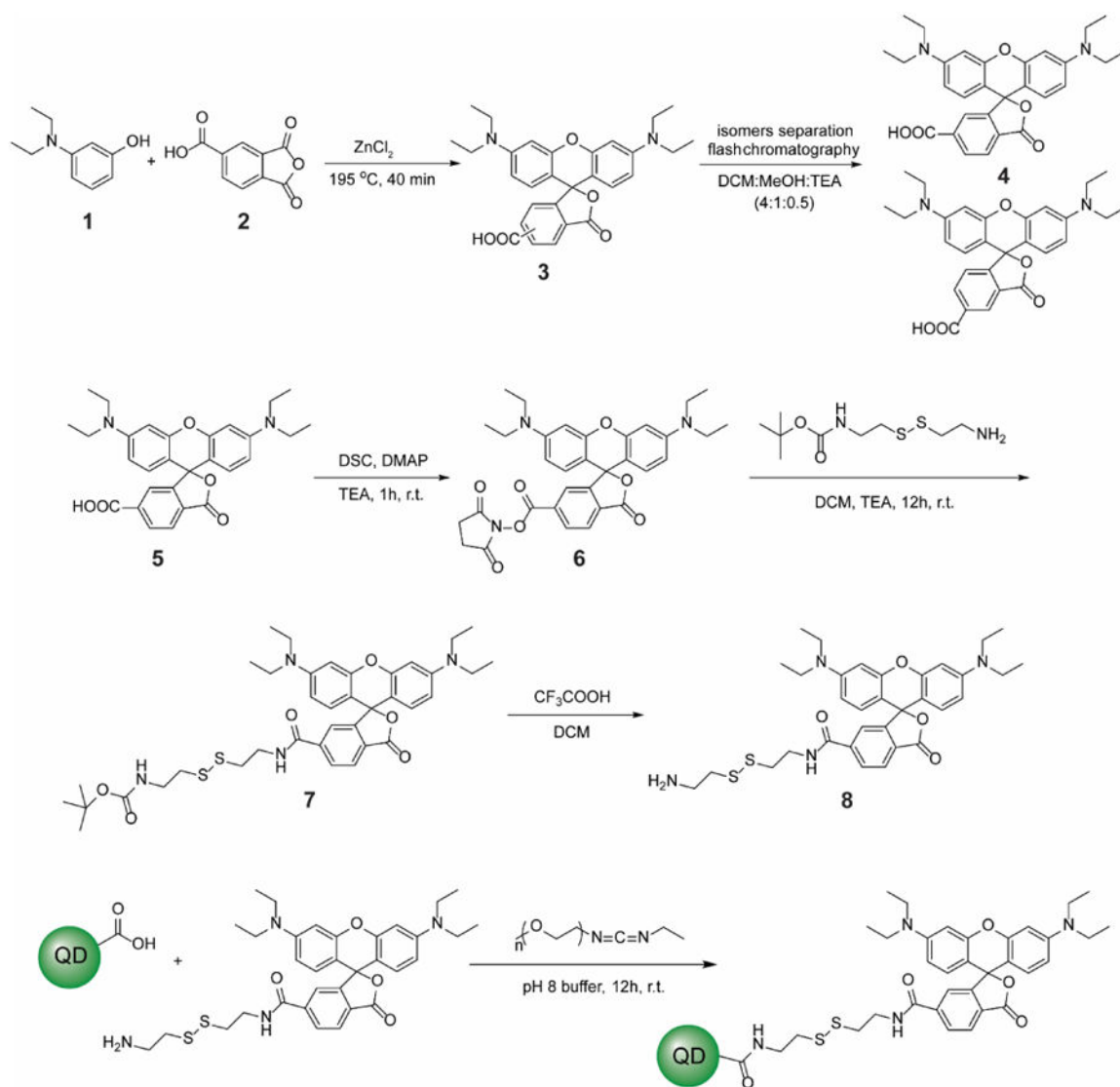


**Figure 3.** Two sets of fluorescence images of  $\text{HS}^-$  detection in HeLa cells. The cells are imaged with optical filters to separately measure the donor QD vs. dye acceptor emissions as labeled in the figures. Before: Image prior to sodium sulfide addition. After: The same after exposure to sodium sulfide solution.



**Scheme 1.**  
Mechanism of the ratiometric response of the sensor based on FRET modulation.



**Scheme 2.**

Synthesis of the bisulfide-reactive carboxyrhodamine B dye, and subsequent conjugation to water-soluble QDs.